

Čech Complex Generation with Homotopy Equivalence Framework for Myocardial Infarction Diagnosis using Electrocardiogram Signals

Srikireddy Dhanunjay Reddy, Pujayita Deb, Tharun Kumar Reddy Bollu

Abstract—Early and optimal identification of cardiac anomalies, especially Myocardial infarction (MCI) can aid the individual in obtaining prompt medical attention to mitigate the severity. Electrocardiogram (ECG) is a simple non-invasive physiological signal modality, that can be used to examine the electrical activity of heart tissue. Existing methods for MCI detection mostly rely on the temporal, frequency, and spatial domain analysis of the ECG signals. These conventional techniques lack in effective identification of cardiac cycle inter-dependency during diagnosis. Hence, there is an emerging need for incorporating the underlying connectivity of the intra-session cardiac cycles for improved anomaly detection. This article proposes a novel framework for ECG signal analysis and classification using persistent homological features through Čech Complex generation with homotopy equivalence check, by taking the above-mentioned emerging needs into account. Homological features like persistent birth-death rates, betti curves, and persistent entropy provide transparency of the regional and cardiac cycle connectivity when combined with Machine Learning (ML) models. The proposed framework is assessed using publicly available datasets (MIT-BIH and PTB), and the performance metrics of machine learning models indicate its efficacy in classifying Normal Sinus Rhythm (NSR), MCI, and non-MCI subjects, achieving a 2.8% mean improvement in AUC (area under the ROC curve) over existing approaches.

Index Terms—Electrocardiogram (ECG), Čech complex, Homotopy equivalence, Persistent homological features.

I. INTRODUCTION

ECG is a wearable non-invasive technique for monitoring and detecting cardiac anomalies through the electrical activity of heart tissue [1] [2]. MCI is one of the most challenging cardiovascular diseases (CVD) leading to heart tissue failures and cardiac arrests [1]. Timely automated prediction of the MCI condition can help health practitioners in reducing the mortality rate due to MCI severity [3]. The presence of artifacts and the non-stationarity nature of ECG signal demands prominent feature extraction and robust anomaly detection. Early works used various artifact removal and feature extraction methods prior to classification [4]-[12]. Application of ML models and deep learning (DL) frameworks using raw ECG signals and its extracted features became the traditional and effective combination for CVD prediction [13] [14].

Topological Data Analysis (TDA) is an emerging technique, to analyze the connectivity and complexity of multi-channel physiological signals [15]. Persistent homological features of homological groups using simplicial complex generation serves as robust biomarkers in finding inter-trial connectivity [16] [17]. Distribution and equivalence of point cloud data points affect simplicial complex evolution and obtained features. Homotopy equivalence verification of the generated complex helps reduce outlier effects on other data points [18].

The retrieved features can be provided to the ML models for the targeted task of anomaly detection.

Feature Extraction is a crucial step in recognizing the underlying connectivity patterns of the signal data. In contrast, the homological features derived during the formation of the simplicial complex illustrate the interconnection among the data points in the point cloud, which includes the subject's trial data. This letter analyzes the efficiency of the proposed Čech complex framework in anomaly prediction, relative to existing automated CVD prediction approaches. The primary contributions to this effect are as follows:

- To the best of our knowledge, through this article, a novel Čech complex framework is proposed to classify the ECG signals by an analysis of the connectivity among intra-session trials using persistent homological features.
- Homotopy equivalence checking condition is proposed to nullify the impact of the outliers in point clouds, without removing its significance in Čech complex generation.

Furthermore, the methods that have been proposed are explored in Section II. Within Section III, a description of the datasets is provided. Finally, the results and conclusion are discussed in Sections IV and V.

II. PROPOSED METHOD

A. Čech Complex Generation

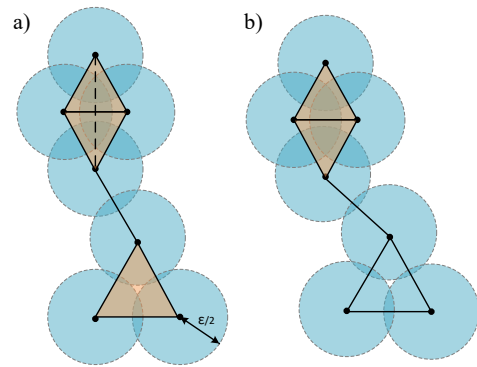


Fig. 1. a) Vietoris-Rips and b) Čech complexes comparison of non-empty intersection

Consider a point cloud $P = \{p_1, p_2, p_3, \dots, p_k\}$, representing K finite set of data points in d -dimensional metric or topological space, where each $p_i \in \mathbb{R}^d$. For the data points p_i and p_j , $\delta(p_i, p_j)$ denotes the distance between these points.

$$\delta(p_i, p_j) = \|p_i - p_j\|^2 = \sqrt{\sum_{k=1}^K (p_i^k - p_j^k)^2} \quad (1)$$

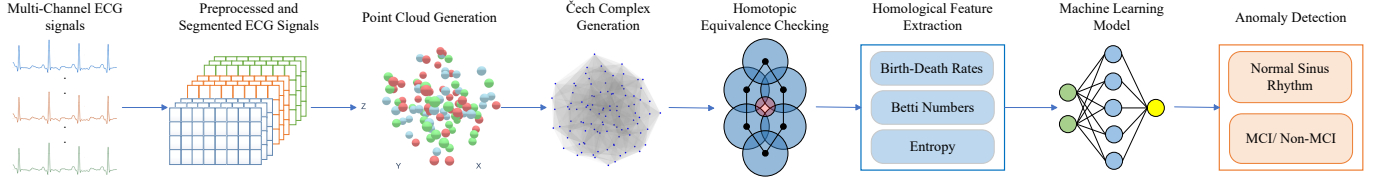


Fig. 2. Čech complex framework for multi-channel ECG signal classification with homotopy equivalence check

To generate Čech complex $\check{C}_\epsilon(P)$ for the given P , an open ball $B_\epsilon(p_i)$ of diameter ϵ is constructed around each p_i . Where $B_\epsilon(p_i)$ is defined as:

$$B_\epsilon(p_i) = \{x \in \mathbb{R}^d; \delta(p_i, x) = \frac{\epsilon}{2}\} \quad (2)$$

x denotes any points on the ball circumference. $\check{C}_\epsilon(P)$ at scale $\frac{\epsilon}{2}$ is constructed by looking at intersection of $B_\epsilon(p_i); \forall i$. 0-simplex (point), 1-simplex (edge), 2-simplex (triangle), 3-simplex (tetrahedron), and their higher-order simplices are the building blocks of $\check{C}_\epsilon(P)$. 0-simplex is formed by each p_i in P . 1-simplex is formed between two points p_i and p_j , if the boundaries of $B_\epsilon(p)$ intersects.

$$B_\epsilon(p_i) \cap B_\epsilon(p_j) \neq \phi, \iff \delta(p_i, p_j) \leq \epsilon \quad (3)$$

Similarly, to form the $K - 1$ simplex, corresponding $B_\epsilon(p)$ has to follow the non-empty intersection condition as follows:

$$\bigcap_{k=1}^K B_\epsilon(p_k) \neq \phi, \iff \delta(P) \leq \epsilon \quad (4)$$

Formally, $\check{C}_\epsilon(P)$ at scale $\frac{\epsilon}{2}$ is the set of simplices σ formed by the point cloud P , that can be denoted as:

$$\check{C}_\epsilon(P) = \{\sigma \subset P : \bigcap_{P \in \sigma} B_\epsilon(P) \neq \phi\} \quad (5)$$

$\check{C}_\epsilon(P)$ can be generated with the evolution of the $B_\epsilon(p_i); 0 \rightarrow \epsilon$. considering the evolution of the $\check{C}_\epsilon(P)$ with different ball radii set $\{\epsilon_1, \epsilon_2, \epsilon_3, \dots, \epsilon_m\}$, the relation among the complexes at different ϵ values are given as follows:

$$\check{C}_{\epsilon_1}(P) \subseteq \check{C}_{\epsilon_2}(P) \subseteq \check{C}_{\epsilon_3}(P) \subseteq \dots \check{C}_{\epsilon_m}(P) \quad (6)$$

With the condition being $\epsilon_1 < \epsilon_2 < \epsilon_3 < \dots < \epsilon_m$. Figure 1 shows the example of generated Vietoris-Rips and Čech complexes comparison with limited data points. The generation strategy of the multi-channel physiological signal is discussed in [21] (section 2.2). From figure 1, it can be observed that the Vietoris-Rips complex has more homological groups when compared to Čech complex. Additional 2-simplex and 3-simplex are formed in the Vietoris-Rips complex without satisfying the requirement of a non-empty intersection, which may result in homotopy inequivalence. The corresponding data points meet the distance metric condition but fail to satisfy the non-empty condition in (4). Subsequent sections will address the significance and applications of homotopy equivalence.

B. Homotopy Equivalence Check

Generated Čech complex is said to be homotopically equivalent if it can be transformed into the union of $B_\epsilon(P)$ without

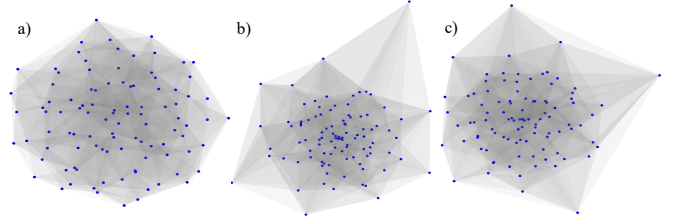


Fig. 3. Generated Čech complexes for a) NSR, b) MCI, and c) non-MCI subjects

tearing or gluing using new points. Consider mapping functions as shown below:

$$f : \check{C}_\epsilon(P) \rightarrow \bigcup_{k=1}^K B_\epsilon(p_k) \quad (7)$$

$$g : \bigcup_{k=1}^K B_\epsilon(p_k) \rightarrow \check{C}_\epsilon(P) \quad (8)$$

Then, mapping functions f and g satisfies the equivalent condition:

$$f \circ g \simeq g \circ f \simeq id_P \quad (9)$$

' \circ ' represents the composition of two maps, and ' id_P ' represents identical mapping on topological space. In addition to this mapping condition, if $\check{C}_\epsilon(P)$ satisfies the following non-empty contradiction condition, then the generated Čech complex is homotopically equivalent.

$$\bigcap_{k=1}^K B_\epsilon(p_i) \neq \phi \quad (10)$$

Figure 3 shows $\check{C}_\epsilon(P)$ of different classes of subjects that exist in datasets used in this article. It has been noted that P associated with MCI and non-MCI exhibits outliers, indicating an unequal distribution of data points. The homotopy equivalence criterion will maintain the significance of these data points, and their effects can be mitigated by eliminating the transient simplex feature data.

C. Persistent Homological Features

Homological features describe the evolution of the Čech complex with various ϵ values. In this process, homological groups, connected components (H_0), loops (H_1), and voids (H_2) are generated. Connected simplices are the building blocks of these homological groups. Features like birth-death rates (b, d), betti curves $\beta_i(\epsilon)$, and entropy of simplices E are used as the measure on connectivity among trials. Expression of these features concerning (b, d) can be noted as follows:

$$f(b, d) = \{(b, d] : b, d \in \mathbb{R}\} \cup \{b, \infty : b \in \mathbb{R}\} \quad (11)$$

TABLE I
 E_μ AND E_{σ^2} COMPARISON OF NSR, MCI, AND NON-MCI FOR ALL
 HOMOLOGICAL GROUPS

E	NSR			MCI			non-MCI		
	H0	H1	H2	H0	H1	H2	H0	H1	H2
E_μ	0.35	0.28	0.32	0.55	0.6	0.57	0.5	0.53	0.51
E_{σ^2}	0.05	0.04	0.02	0.12	0.14	0.16	0.1	0.11	0.09

$$\beta_k(\epsilon) = \sum_{k=1}^K w(b-d) \vec{1}_k \quad (12)$$

$$E = \sum_{k=1}^K \frac{d_k - b_k}{L} \log\left(\frac{d_k - b_k}{L}\right); L = \sum_{k=1}^K (d_k - b_k) \quad (13)$$

$f(b, d)$ represents the linear representation function of birth-death of the homological groups. $\beta_k(\epsilon)$ represents the population of the different homological groups with the evolution of ϵ in terms of increasing monotonic function $w(\cdot)$ and 1's vector. E explains the underlying connectivity of subject-specific sessions concerning homological group evolution. In general, outliers have minimal (b,d) values based on the distance metric. Focusing on groups that persist across a wide range of ϵ evolution, eliminates the shortest living homological features from homotopy equivalent verified Čech complex. Moreover, extracted homological features can be provided to ML models for anomaly prediction.

D. Proposed Čech Complex Framework

Consider ECG signal data $X \in \mathbb{R}^{ch \times s}$ with ch number of channels and s number of time samples per channel. Initially, X is subjected to a two-stage median filter and Discrete Wavelet Transform filtering techniques [3], to remove the myographic and baseline wander contamination from the cardiac signal data. Further, X is segmented into 4-second trials and then vectorized to get $X \in \mathbb{R}^{n \times t}$, n represents the number of trials, and t represents the number of time samples per trial. Now, X is decomposed into the orthonormal vectors U and the eigenvalue matrix Λ as follows:

$$X_{n \times t} = U_{n \times n} \Lambda_{n \times t} U_{n \times n}^T \quad (14)$$

Proposed Čech complex framework generated a three-dimensional point cloud $P \in \mathbb{R}^{n \times 3}$ by selecting the 3 high-ranked eigenvalues (to observe upto third-order homological group distribution). d -dimensional point cloud can be generated for different applications, by mapping the d -eigenvalues of Λ_k onto the appropriate U_d eigenvectors as follows:

$$P = U_k \Lambda_k^{\frac{1}{2}} \quad (15)$$

Further, P is utilized to generate $\check{C}_\epsilon(P)$ under homotopy equivalent condition (10). Persistent homological features like (b, d) , $\beta_k(\epsilon)$, and E of simplices are calculated to do anomaly detection using various ML models. Figure 2, indicates the overall flow of the proposed Čech complex framework.

III. DATASET DESCRIPTION

The proposed Čech complex framework is implemented and validated on the PTB Diagnostic ECG Database (PTB) [19] and MIT-BIH Arrhythmia Database (MIT-BIH AD) [20]. PTB comprises a 2-minute, 15-lead high-resolution ECG signal

data, including 52 NSR, 148 MCI, and 68 non-MCI subject samples, recorded at a sampling frequency of 1000 Hz. In this work, 12 lead ECG data is utilized to validate the proposed framework. Further, ECG signals are processed to eliminate noise and baseline wander before being segmented into 4-second intervals and then homological features are extracted. MIT-BIH AD comprises a 30-minute, 2-lead (V5 and II) 11-bit resolution ECG recording sampled at 360 Hz from 48 participants, featuring labeled sessions of different arrhythmic conditions. In this article, arrhythmic conditions that may lead to Mild Cognitive Impairment (MCI), such as ventricular fibrillation, ventricular tachycardia, atrial fibrillation, and sinus bradycardia, are labeled as MCI. Conversely, conditions including atrial flutter, supraventricular tachycardia, bigeminy, and trigeminy are classified as non-MCI. Further preprocessed and 4-sec segmented trials are passed to the proposed framework.

IV. RESULTS & DISCUSSION

A. Homological feature analysis

Homological features are calculated from the generated Čech complex as discussed in the section II-C. Based on the trial wise (b,d) rate of each homological groups (H_0, H_1, H_2), entropy E of a subject is calculated. Further, mean entropy (E_μ) and entropy variance (E_{σ^2}) of each class homological group is calculated as shown in Table I. Increased E_μ and E_{σ^2} of MCI and non-MCI classes represents the high non-stationarity in comparison with NSR class. In Figure 4, homological features from MSR, MCI, and non-MCI subjects are visualized. (UP) shows the persistent homological plot of all homological groups (b,d) values. (DOWN) shows the Betti curves $\beta_k(\epsilon)$ demonstrating group evolution (b,d). Due to their complex and significant non-stationarities, MCI and non-MCI features overlap more than NSR. The large betti curve distribution for NSR indicates its stable and simpler point cloud structure. Naive MCI and non-MCI distribution imply unstable and complex structures.

B. Myocardial Infraction detection

Extracted homological features from the proposed Čech complex framework are fed to diverse ML models with a 5-fold cross-validation scheme by the 80:20 train-test split strategy. Parameter configuration of the best-performed model details are discussed as follows:

Random Forest: Random Forest classifier was optimized with 275 trees and a max_depth of 21 to balance complexity and performance. The model used a 4 min_samples_split and 3 min_samples_leaf to control overfitting.

SVM: Support Vector Machine (SVM) classifier achieved optimal performance using a Radial Basis Function (RBF) kernel and a regularization parameter (C) of 0.5. The gamma parameter was set to 'scale' to capture data variance.

MLP: ReLU activation enhanced feature learning in a 3-layer Multi-Layer Perceptron (MLP) classifier with 256, 64, and 32 neurons. Using line search, learning rate of 0.001 has used wit ADAM optimized model for efficient convergence. To avoid overfitting, dropout regularization at 0.25 improved classification performance.

Logistic Regression: Logistic Regression model performed

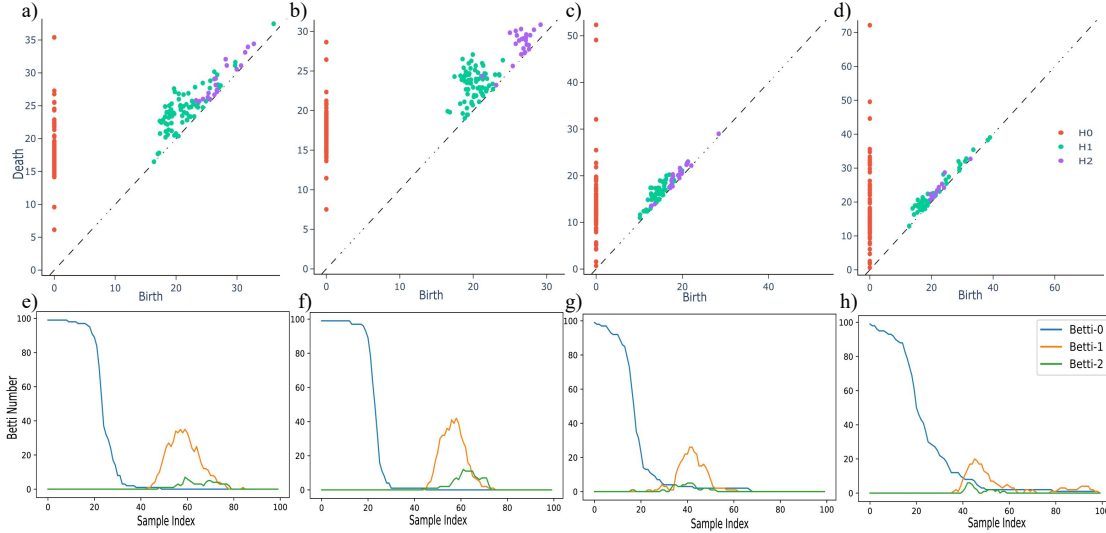


Fig. 4. Homological features comparison; UP: a-b) NSR, c) MCI, and d) non-MCI subject persistent homological data plots; DOWN: e-f) NSR, g) MCI, and h) non-MCI subject betti curve plots

TABLE II
PERFORMANCE COMPARISON OF DIFFERENT MODELS ON PTB [19] AND MITBIH-AD [20] DATASETS USING ČECH COMPLEX FRAMEWORK

Classifiers	NSR Vs MCI								MCI Vs non-MCI								NSR Vs MCI Vs non-MCI							
	Acc±SD		AUC		f1 score		Kappa		Acc±SD		AUC		f1 score		Kappa		Acc±SD		AUC		f1 score		Kappa	
	I	II	I	II	I	II	I	II	I	II	I	II	I	II	I	II	I	II	I	II	I	II	I	II
Random Forest	98.0±1.58	95.2±2.1	0.99	0.98	0.98	0.96	0.94	0.94	96.8±2.0	90.1±2.3	0.98	0.94	0.98	0.91	0.94	0.87	89.7±2.5	85.3±2.9	0.94	0.9	0.93	0.86	0.92	0.82
SVM	95.6±2.3	92.8±2.5	0.94	0.96	0.93	0.94	0.9	0.91	91.5±2.5	88.3±2.6	0.88	0.92	0.86	0.89	0.83	0.85	86.7±2.7	83.9±2.9	0.85	0.88	0.84	0.85	0.8	0.8
MLP	96.3±2.0	93.5±2.4	0.95	0.97	0.94	0.95	0.92	0.92	94.7±2.3	89.4±2.5	0.92	0.93	0.87	0.9	0.88	0.88	87.3±2.4	84.8±2.7	0.91	0.89	0.89	0.86	0.88	0.81
Logistic Regression	94.5±2.5	91.7±2.9	0.93	0.95	0.92	0.93	0.89	0.9	89.3±3.0	86.7±3.1	0.87	0.91	0.85	0.88	0.84	0.86	85.1±2.9	82.6±3.0	0.84	0.87	0.82	0.84	0.78	0.79
Decision Tree	93.1±3.1	90.4±3.2	0.91	0.94	0.9	0.92	0.87	0.88	90.5±3.2	85.2±3.4	0.85	0.89	0.83	0.86	0.86	0.81	83.2±3.4	80.9±3.5	0.82	0.84	0.8	0.83	0.75	0.78

* (ACC±SD) represents Accuracy ± Standard Deviation) value in a percentage format. I and II refers to the datasets [18] → 12-leads and [19] → 2-leads

TABLE III
COMPARISON OF THE PROPOSED FEATURES PERFORMANCE ON PTB DATASET WITH EXISTING METHODS

Approach	Complexity	Classification	F1 score	AUC
U-net [22]	$O(n^2m)$	NSR Vs MCI	92.53	97.96
CNN [23]	$O(n^2md)$	NSR Vs MCI	97.8	96.54
ECG-SMART-NET [24]	$O(n^2md)$	NSR Vs MCI	64.2	92.35
RNN [25]	$O(nm^2h)$	NSR Vs MCI	96.24	97.8
		MCI Vs non-MCI	94.91	96.9
RNN [26]	$O(nm^2h)$	NSR Vs MCI	97.65	98
		MCI Vs non-MCI	96.72	97.24
Wavelet Transform [27]	$O(n^2 \log n)$	NSR Vs MCI	97.14	97.86
Time-Frequency [28]	$O(n^2m)$	NSR Vs MCI	92.53	93.26
Homological Features (proposed)	$O(n^2m)$	NSR Vs MCI	98.97	99.2
		MCI Vs non-MCI	98.67	98.81
		NSR Vs MCI Vs non-MCI	93.12	94.26

* n : no. of trials, m : trial length, d : model depth, h : no. of hidden layers

best with L2 regularization and a regularization strength (C) of 5. The 'lbfgs' solver was used for efficient convergence, and the model required 180 iterations to achieve optimal results.

Decision Tree: Decision Tree classifier was optimized with a max_depth of 15 to avoid overfitting. The model used 3 min_samples_split and 2 min_samples_leaf to control tree complexity. The Gini criterion was employed to determine the best splits.

Table II compares binary and multi-class classification metrics of best performing models on PTB and MITBIH-AD datasets. Comparatively, the proposed framework performs well in NSR Vs MCI classification. Because of the non-stationary similarities between MCI and non-MCI, misclassification happened among these classes, in the other classification tasks. The proposed Čech complex framework provided consistent performance with stabilized standard deviation on 12-lead and 2-lead datasets with varied sampling frequencies and specifications. Table III describes the efficiency of the proposed homological

features performance and complexity in comparison with the existing methods. The approaches utilizing wavelet transform and time-frequency characteristics demonstrate reduced computational cost with minimal performance. Raw ECG signals processed with U-net, CNN, ECG-SMART-NET, and RNN based frameworks yield modest performance accompanied by a considerable cost. Furthermore, the proposed Čech complex framework, incorporating persistent homological properties, contended with other complex models and exhibited 2.8% mean gain in identification task. It also demonstrates proficiency in multi-class categorization with encouraging metric values. Čech complex framework class prediction tasks are evaluated for statistical significance using a paired t-test ($p < 0.02$).

V. CONCLUSION

In this letter, for the first time, a novel Čech complex approach is proposed to utilize the persistent homological features for classifying NSR, MCI, and non-MCI subjects using ECG signals. The proposed framework captures the connectivity among the intra-session trials using homological groups evolved in the generation of Čech complex. Further, the homotopy equivalence checking condition nullifies the impact of outliers in the simplices generation while preserving their significance in feature extraction. The performance of ML models demonstrates the efficacy of homological features in both binary and multi-class classification. Further, this TDA approach can be extended with techniques like two-dimensional warping and shallow network schemes for more effective comprehension of the complexities between MCI and non-MCI ECG trials [29] [30].

REFERENCES

- [1] D.H. Brooks and R.S. MacLeod, 1997. "Electrical imaging of the heart". *IEEE Signal Process. Mag.*, 14(1), pp.24-42.
- [2] S. Kanna, et al., 2018. "Bringing wearable sensors into the classroom: A participatory approach". *IEEE Signal Process. Mag.*, 35(3), pp.110-130.
- [3] "Fact sheet on CVDs", World Health Organization (WHO), Geneva, Switzerland, 2017.
- [4] I.H.S. Markit, 2017. "The complexities of physician supply and demand: Projections from 2015 to 2030". *Association of American Medical Colleges*.
- [5] S.D. Reddy, et al., 2023. "Classification of arrhythmia disease through electrocardiogram signals using sampling vector random forest classifier". *Multimedia Tools and Applications*, 82(17), pp.26797-26827.
- [6] A.K. Roonizi, 2020. "A new approach to Gaussian signal smoothing: Application to ECG components separation". *IEEE Signal Process. Lett.*, 27, pp.1924-1928.
- [7] H. Chen, et al., 2021. "CLECG: A novel contrastive learning framework for electrocardiogram arrhythmia classification". *IEEE Signal Process. Lett.*, 28, pp.1993-1997.
- [8] V.G. Sirtoli, et al., 2023. "Removal of motion artifacts in capacitive electrocardiogram acquisition: A review". *IEEE Transactions on Biomedical Circuits and Systems*, 17(3), pp.394-412.
- [9] A. Mondal, M.S. Manikandan, and R.B. Pachori, 2024. "Automatic ECG Signal Quality Determination Using CNN with Optimal Hyperparameters for Quality-Aware Deep ECG Analysis Systems". *IEEE Sens. J.*
- [10] G. Revach, et al., 2024. "HKF: Hierarchical Kalman Filtering With Online Learned Evolution Priors for Adaptive ECG Denoising". *IEEE Trans. Signal Process.*
- [11] C. Uhl, et al., 2020. "Subspace detection and blind source separation of multivariate signals by dynamical component analysis (DyCA)". *IEEE OJSP*, 1, pp.230-241.
- [12] R. Song, et al., 2022. "Video-based heart rate measurement against uneven illuminations using multivariate singular spectrum analysis". *IEEE Signal Process. Lett.*, 29, pp.2223-2227.
- [13] H. Chen, et al., 2021. "CLECG: A novel contrastive learning framework for electrocardiogram arrhythmia classification". *IEEE Signal Process. Lett.*, 28, pp.1993-1997.
- [14] U. Satija, J. Mathew, and R.K. Behera, 2022. "A unified attentive cycle-generative adversarial framework for deriving electrocardiogram from seismocardiogram signal". *IEEE Signal Process. Lett.*, 29, pp.802-806.
- [15] X. Xu, N. Drougard, and R.N. Roy, 2021. "Topological data analysis as a new tool for EEG processing". *Frontiers in Neuroscience*, 15, p.761703.
- [16] S.D. Reddy and T.K. Reddy, 2024. "Delaunay Triangulated Simplicial Complex Generation for EEG Signal Classification". *IEEE Sens. Lett.*
- [17] S.D. Reddy, T.K. Reddy, and H. Higashi, 2024, February. "Chromatic Alpha Complex Generation for EEG Signal Classification". *National Conference on Communications (NCC)* (pp. 1-5). IEEE.
- [18] F. Chazal and B. Michel, 2021. "An introduction to topological data analysis: fundamental and practical aspects for data scientists". *Frontiers in artificial intelligence*, 4, p.667963.
- [19] R. Bousseljot, D. Kreiseler, and A. Schnabel, 1995. "Nutzung der EKG-Signaldatenbank CARDIODAT der PTB über das Internet".
- [20] G.B. Moody and R.G. Mark, 2001. "The impact of the MIT-BIH arrhythmia database". *IEEE engineering in medicine and biology magazine*, 20(3), pp.45-50.
- [21] S.D. Reddy and T.K. Reddy, 2024, April. "GM-VRC: Semantic Topological Data Ensemble Approach for EEG Signal Classification". In *ICASSP 2024-2024 IEEE International Conference on Acoustics, Speech and Signal Processing (ICASSP)* (pp. 1971-1975). IEEE.
- [22] P.S. Choudhary and S. Dandapat, 2024. "Morphology-Aware ECG Diagnostic Framework with Cross-Task Attention Transfer for Improved Myocardial Infarction Diagnosis". *IEEE T. Instrum. Meas.*
- [23] U.B. Baloglu, et al., 2019. "Classification of myocardial infarction with multi-lead ECG signals and deep CNN". *Pattern recognition letters*, 122, pp.23-30.
- [24] N.T. Riek, et al., 2024. "ECG-SMART-NET: A Deep Learning Architecture for Precise ECG Diagnosis of Occlusion Myocardial Infarction". arXiv preprint arXiv:2405.09567.
- [25] E. Prabhakararao and S. Dandapat, 2020. "Myocardial infarction severity stages classification from ECG signals using attentional recurrent neural network". *IEEE Sens. J.*, 20(15), pp.8711-8720.
- [26] E. Prabhakararao and S. Dandapat, 2020. "Attentive RNN-based network to fuse 12-lead ECG and clinical features for improved myocardial infarction diagnosis". *IEEE Signal Process. Lett.*, 27, pp.2029-2033.
- [27] M. Kumar, R.B. Pachori, and U.R. Acharya, 2017. "Automated diagnosis of myocardial infarction ECG signals using sample entropy in flexible analytic wavelet transform framework". *Entropy*, 19(9), p.488.
- [28] I. Kayikcioglu, et al., 2020. "Time-frequency approach to ECG classification of myocardial infarction". *Computers & Electrical Engineering*, 84, p.106621.
- [29] T. Meyer, et al., 2024. "Time Scale Network: An Efficient Shallow Neural Network For Time Series Data in Biomedical Applications". *IEEE Journal of Selected Topics in Signal Processing*.
- [30] M. Schmidt, et al., 2014. "Two-dimensional warping for one-dimensional signals—conceptual framework and application to ECG processing". *IEEE Trans. Signal Process.*, 62(21), pp.5577-5588.